Supporting data

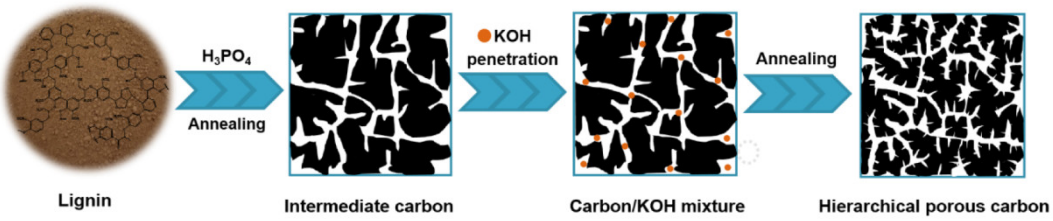

Figure S1. Schematic representation of the synthetic strategy of lignin-derived OHPC.

Figure S1 illustrated the detailed synthetic strategy of lignin-derived OHPCs. Firstly, lignin as carbon source was thoroughly immersed into H_3PO_4 aqueous solution. After dried, the mixture was annealed at 400 °C for 1 h to obtain IC. Subsequently, the IC was homogeneously mixed with KOH solution, followed by heat treatment under a N_2 atmosphere to form lignin-derived OHPCs. Actually, the initial H_3PO_4 pre-treatment played positive advantage in subsequent KOH activation process and effectively leaded to the formation of OHPCs. Concretely, the H_3PO_4 assistants cross-linked with lignin sources and generated phosphate (and/or polyphosphate) esters groups throughout the lignin structure, which endowed the pre-activated IC with hierarchical porous structure. In addition, the IC also inherited rich oxygen-containing groups as shown in Figure S4. During subsequent KOH activation, such multi-scale porous structure and abundant oxygen species of IC collectively improved the wettability between IC and KOH solution and facilitated the evolution of pore morphologies, eventually forming the lignin-derived OHPCs. The formation of phosphate groups and the role of pre-treatment in subsequent KOH activation was systemically discussed in supplemental materials.

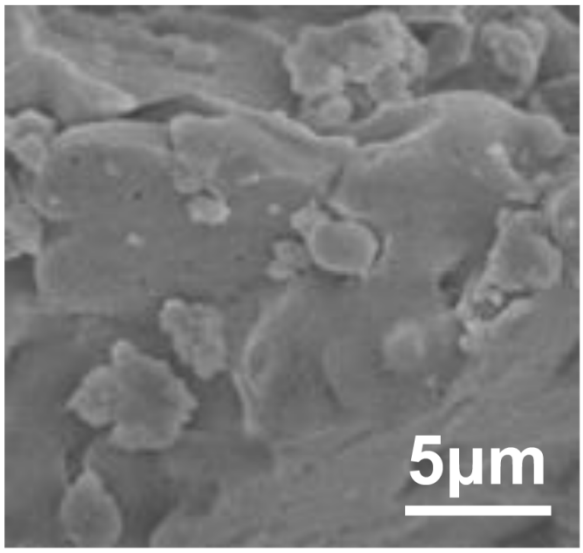

Figure S2. SEM image of the raw lignin particles.

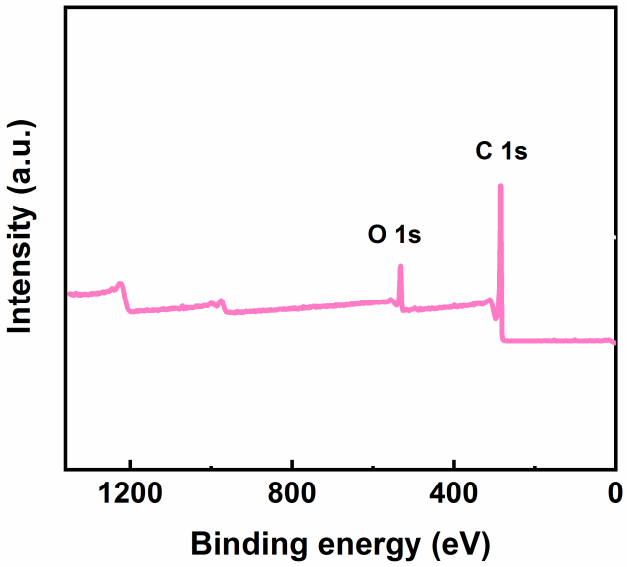

Figure S3. XPS survey spectrum of OHPC.

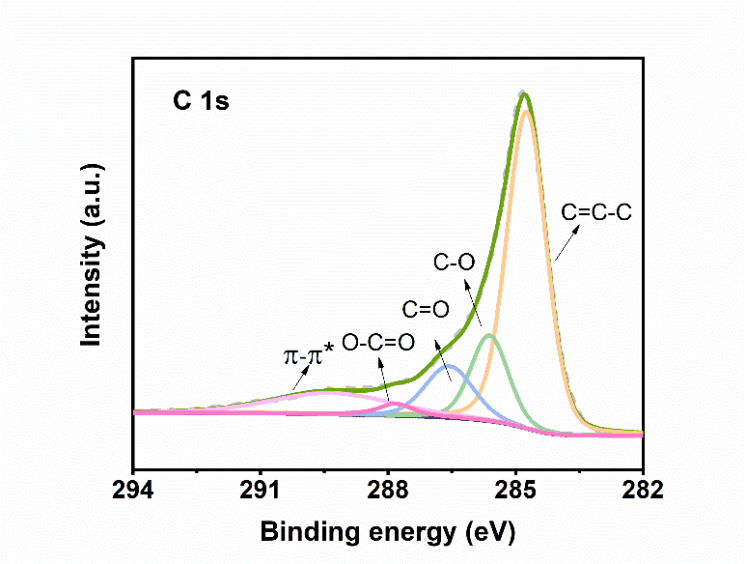

Figure S4. High-resolution C1s XPS spectrum of OHPC material.

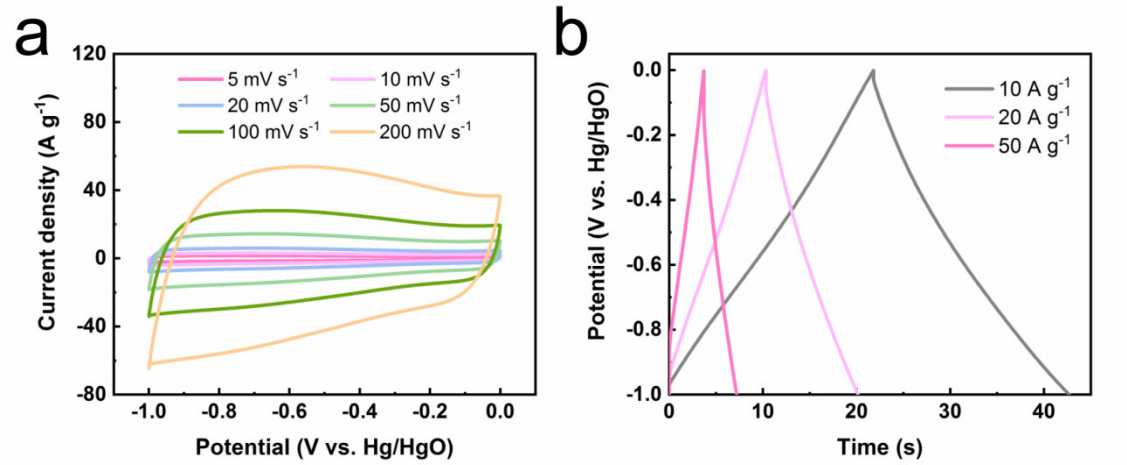

Figure S5. (**a**) The rate-dependent CV curves of OHPC at scan rates varied from 5 to 200 mV s^{-1}. (**b**) The GCD profiles of OHPC at different rate from 10 A g^{-1} to 50 A g^{-1}.

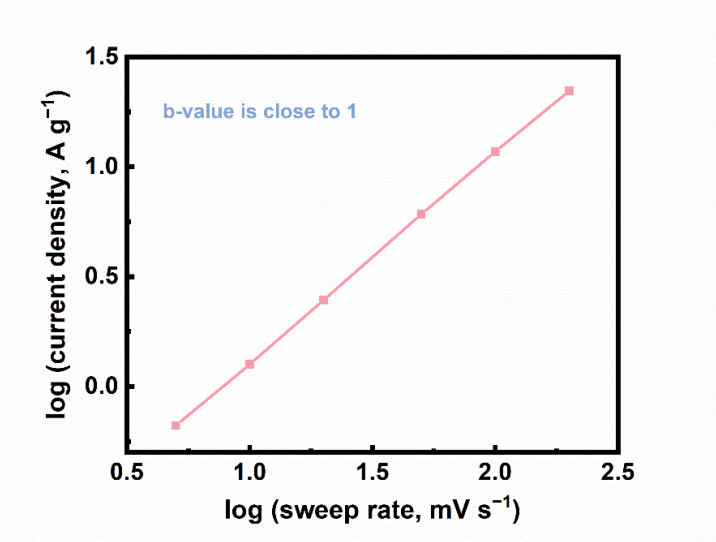

Figure S6. b-value determination of the anodic peak current density shows that this value is approximately 1.

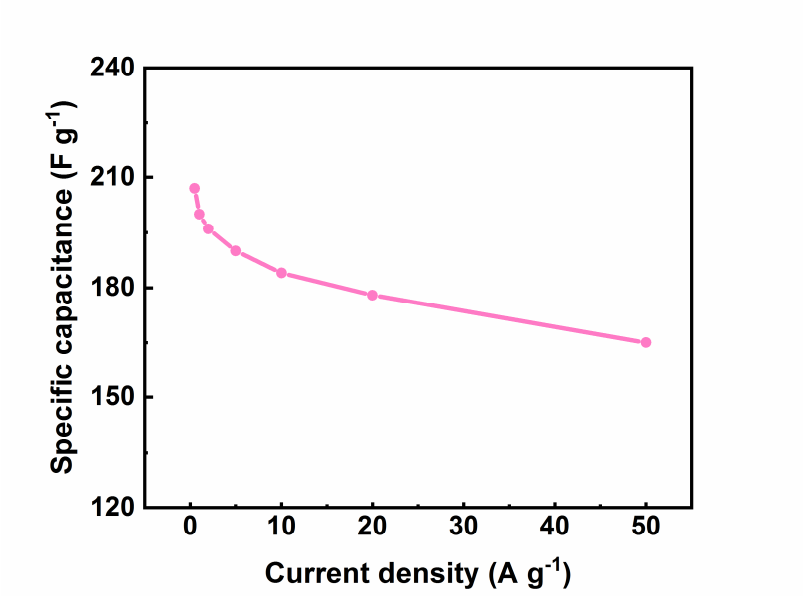

Figure S7. The capacitance performance of the porous carbon electrode by direct KOH activation of lignin at 700 °C.

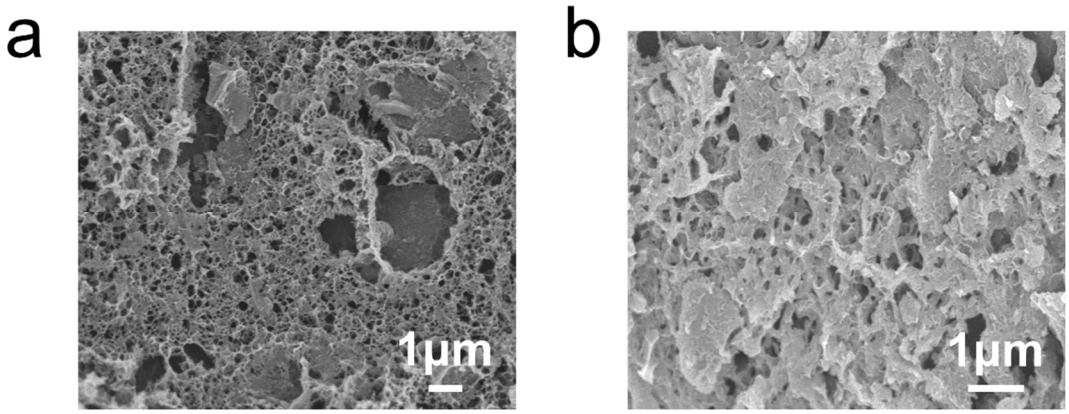

Figure S8. The SEM images of lignin-derived hierarchical porous carbon calcinated at different temperatures (**a**) 800 °C and (**b**) 900 °C.

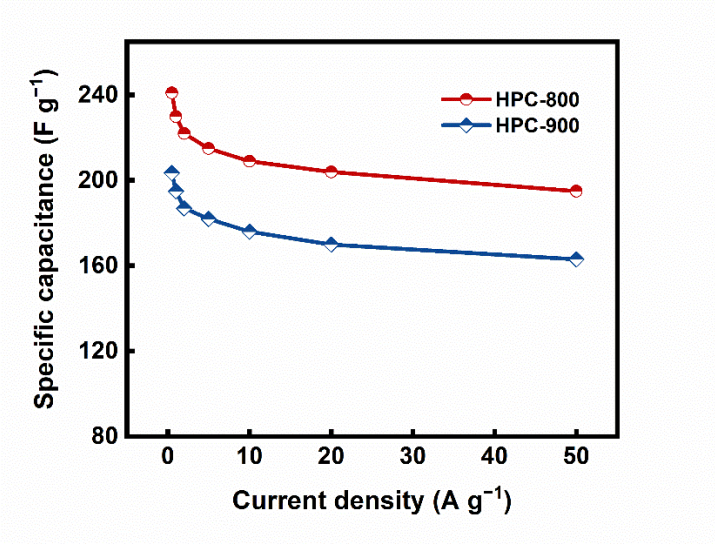

Figure S9. The gravimetric rate performance of lignin-derived hierarchical porous carbon calcinated at 800 °C and 900 °C from 0.5 to 50 A g^{-1}.

Table S1. The element concentration of OHPC sample.

Elements	Concentration (%)
C	89.22
O	10.78

Table S2. Comparison of electrochemical performances for the lignin-based carbon materials.

Electrode	precursor	Specific surface area ($m^2\ g^{-1}$)	Mass loading	Voltage window (V)	Electrolyte	Specific capacitance ($F\ g^{-1}$)	Rate capability	E ($W\ h\ kg^{-1}$) (P ($KW\ kg^{-1}$))	References
PGBC[a]	Bamboo char	1732	4.8 mg	3.0	KOH/PVA	222.0 at 0.5 A g^{-1}	51.8% at 20 A g^{-1}	6.68 (0.1)	[60]
HOMC[b]	Walnut shell lignin	2033	2.4 mg	0–1.0	6 M KOH	286 at 0.2 A g^{-1}	72.1% at 20 A g^{-1}	13.5 (44.3)	[58]
Porous carbons	Lignin	3065	3 mg	0–1.0	6 M KOH	325 at 0.5 A g^{-1}	80.8% at 50 A g^{-1}	8.1 (0.1)	[37]
Porous carbon	Oxidized lignin	3094	-	0–1.0	6 M KOH	352.9 at 0.5 A g^{-1}	82.7% at 10 A g^{-1}	9.5 (0.025)	[52]
PCS[c]	Sodium lignosulphonate	1372.87	5 mg	0–1.0	3 M KOH	340 at 0.5 A g^{-1}	72% at 10 A g^{-1}	9.7 (0.25)	[62]
CAs[d]	lignin	1681.6	-	0–1.0	1 M H_2SO_4	260.3 at 1.0 A g^{-1}	60.7% at 20 A g^{-1}	26.25 (1.0)	[63]
N, S-HPC[e]	Sodium lignosulfonate	1454.7	-	0–1.0	6 M KOH	269 at 0.5A g^{-1}	62% at 50 A g^{-1}	37.4 (0.062)	[54]
lignin/PAN nanofiber	Alkali lignin	1176.0	-	0–1.0	lignin hydrogel in 3.3 M KOH	-	-	4.49 (0.252)	[61]
Porous carbon	Alkali lignin	1831	2.5 mg cm^{-2}	0-1.0	6 M KOH	□428 at 1.0 A g^{-1}	82.9% at 30 A g^{-1}	66.18 (0.312) in EMIM TFSI	[36]
LCNFs[f]	Melon seed shells and peanut shells	1254.5	-	-1.6-0	1 M Na_2SO_4	533.7 at 0.25 A g^{-1}	90.6% at 10 A g^{-1}	69.7 (0.78)	[56]

CNFs[g]	Softwood Kraft lignin	1124	2.212 mg cm^{-2}	0-0.8	6 M KOH	103.6 at 0.25 A g^{-1}	58.2 at 4 A g^{-1}	-	[57]
Carbon aerogels	Softwood kraft lignin	1,609	-	0-1.0	1.0 H_2SO_4	122 at 1.0 A g^{-1}	46.4% at 1A g^{-1}	3.2 (0.209)	[53]
Carbon nanofibers	Lignin/PVA blend (80:20)	2170	-	3.5	$Pyr_{14}TFSI$	87 at 1.0 A g^{-1}	-	38 (1.67)	[59]
LCNFs-PRL[h]	Poplar	1062.5	-	0-1.0	6 M KOH	349.2 at 1.0 A g^{-1}	85.4% at 5A g^{-1}	56.9 (0.4) in 1 M Na_2SO_4	[55]
OHCP	Industrial lignin	1289.7	1.5-2.0 mg cm^{-2}	0-1.0	6 M KOH	258 F g^{-1} at 0.5 A g^{-1}	80% at 50 A g^{-1}	9.27 (0.025)	This work

[a] Three-dimensional porous graphitic biomass carbon

[b] Ordered mesoporous carbons (OMCs) with hierarchical pore structure

[c] Porous carbon spheres

[d] Carbon aerogels (CAs) with hierarchically porous morphologies

[e] Three-dimensional interconnected nitrogen and sulfur codoped porous carbon materials

[f] Light-weight lignin-based carbon nanofibers

[g] Freestanding nonwoven carbon fiber

[h] Poplar lignin (PRL) based lignin-based carbon nanofibers